RSC Advances

PAPER

View Article Online
View Journal | View Issue

Open Access Article. Published on 03 March 2025. Downloaded on 11/8/2025 10:29:35 PM.
This article is licensed under a Creative Commons Attribution-NonCommercial 3.0 Unported Licence.

Check for updates

Cite this: *RSC Adv.*, 2025, **15**, 6931

Colorimetric sensor for Pb^{2+} detection in water using thioglycolic acid-conjugated gold nanoparticles

Febrina Amelia Saputri, *[a] Talitha Shabirah Aulia,[a] Catur Jatmika,[a] Raditya Iswandana,[b] Sandra Megantara[c] and Vinayak A. Dhumale[d]

Environmental pollution by the heavy metal lead (Pb^{2+}) poses significant health risks, including kidney damage and neurotoxicity in children. Gold nanoparticles (AuNPs) have shown promise as colorimetric sensors for visually detecting Pb^{2+} through surface plasmon resonance. This study developed a colorimetric method using thioglycolic acid (TGA) as a conjugate, leveraging its strong S–Au bond and carboxyl group to enhance AuNPs stability and Pb^{2+} specificity. The method was optimized and examined using UV-visible spectrophotometry, High-Resolution Transmission Electron Microscopy (HRTEM), and Fourier Transform Infrared Spectroscopy (FTIR). Optimal conditions were identified as 700 μL AuNPs, 500 μM thioglycolic acid, and pH 10.0 for 10 minutes. The synthesized TGA-AuNPs could detect Pb^{2+} at a limit of 9.5 μg mL^{-1}. The sensor demonstrated specificity to Pb^{2+} against Ba^{2+}, Mn^{2+}, Cu^{2+}, Mg^{2+}, and Hg^{2+}. The application to water samples from Lake Kenanga, Puspa, and FMIPA in Universitas Indonesia indicated that Pb^{2+} levels were below the detectable concentration. This research successfully developed a simple, fast, cost-effective TGA-AuNPs colorimetric sensor for real-time Pb^{2+} detection in water.

Received 30th August 2024
Accepted 22nd February 2025

DOI: 10.1039/d4ra06260d

rsc.li/rsc-advances

1 Introduction

Environmental pollution from heavy metals, particularly lead (Pb^{2+}), poses significant health risks due to its bioaccumulation and non-degradable nature.[1,2] Pb^{2+} contamination primarily originates from industrial activities and can result in high blood pressure, cardiovascular issues, kidney damage in adults, and neurotoxicity in children.[2] Recent studies in Indonesia have shown dangerous levels of Pb^{2+} in water sources, emphasizing the need for effective detection methods.[3,4]

Methods like atomic absorption spectrometry (AAS) and inductively coupled plasma mass spectrometry (ICP/MS) are accurate but costly and complex.[5] Colorimetric analysis using gold nanoparticles (AuNPs) offers a simpler, faster, and cost-effective alternative. AuNPs are sensitive to Pb^{2+} due to their surface plasmon resonance (SPR) properties. These characteristics make AuNPs highly sensitive to size, shape, surrounding media, and interparticle distance changes. Metal ions, such as Pb^{2+}, can bind to the surface of AuNPs, inducing aggregation and causing a color change from red to blue.[6–8]

Thiol-conjugated gold nanoparticles have been extensively used due to their long-term stability and high extinction coefficients.[9] Thiol and carboxylate groups, such as those in 11-mercaptoundecanoic acid (11-MUA) and glutathione, have proven effective in detecting Pb^{2+} with AuNPs, achieving detection limits of 400 μM (82.88 μg mL^{-1}) and 100 nM (20.72 μg L^{-1}), respectively.[10,11] However, the detection limits reported in these studies are still relatively high and do not meet the stringent requirements set by international health organizations like the Environmental Protection Agency, which is 15 μg L^{-1}.[12]

Thioglycolic acid ($HSCH_2COOH$) is structurally similar to 11-MUA ($HS(CH_2)_{10}CO_2H$), differing primarily in the length of their alkyl chains. This difference affects solubility, which can influence colorimetric results in aqueous solutions.[9] Thioglycolic acid (TGA) is more readily available and cost-effective than 11-MUA. Environmentally, TGA is considered free of persistent, bioaccumulative, and toxic components, making it suitable for use.[13] In addition to the advantages and ability of TGA to conjugate to AuNPs, there has been no experiment using AuNPs-conjugated TGA to detect Pb^{2+}. This study aims to develop a TGA-conjugated AuNPs colorimetric sensor for real-time Pb^{2+} detection in water, providing an accessible and efficient solution for environmental monitoring.

[a]Laboratory of Pharmaceutical-Medicinal Chemistry and Bioanalysis, Faculty of Pharmacy, Universitas Indonesia, Depok 16424, Indonesia. E-mail: febrina.amelia@farmasi.ui.ac.id

[b]Laboratory of Pharmaceutics and Pharmaceutical Technology, Faculty of Pharmacy, Universitas Indonesia, Depok 16424, Indonesia

[c]Department of Pharmaceutical Analysis and Medicinal Chemistry, Faculty of Pharmacy, Universitas Padjadjaran, Jatinangor 45363, Indonesia

[d]Department of Applied Science and Humanities, School of Engineering and Science, MIT Art, Design and Technology University, Pune 412201, India

© 2025 The Author(s). Published by the Royal Society of Chemistry

Open Access Article. Published on 03 March 2025. Downloaded on 11/8/2025 10:29:35 PM.
This article is licensed under a Creative Commons Attribution-NonCommercial 3.0 Unported Licence.

2 Materials and methods

2.1. Materials and reagents

The main chemicals used were gold nanoparticles with a diameter of 10 nm (Sigma Aldrich, USA) and thioglycolic acid (Sigma Aldrich, USA). Other chemicals included glycine, NaOH (Sigma Aldrich, USA), metal salts $Pb(NO_3)_2$, $BaCl_2$, $Mg(OH)_2$, $CuSO_4$, and $MnCl_2$ (Merck, Germany), $HgCl_2$ (Smartlab, Indonesia), HNO_3 (Merck, Germany), and demineralized water. Water samples in this study were taken from lakes at Universitas Indonesia, including Kenanga Lake, Puspa Lake, and FMIPA Lake.

2.2. Instruments

The UV-visible absorption spectrum was recorded in a quartz cuvette using a UV-visible spectrometer (Thermo Scientific, USA). Functional groups on the surface of AuNPs were identified by Fourier Transformed Infrared spectroscopy (Shimadzu, Japan). The morphology and particle size distribution of TGA-AuNPs were measured with a high-resolution transmission electron microscope (HRTEM) (Tecnai G2 F20 S-TWIN, USA).

2.3. Characterization of AuNPs pre- and post-treatment

As much as 700 μL of untreated AuNPs was mixed with 1 mL of distilled water and incubated for 1 hour, and its absorbance was measured over 400–800 nm.[14] Post-treatment, 700 μL of 10 nm AuNPs was mixed with 1 mL of pH 10.0 glycine–NaOH buffer, 50 μL of 500 μM TGA, and of 1 μM Pb^{2+}, incubated for 1 hour, and absorbance was measured over 400–800 nm.[15]

2.4. Method optimization

Different volumes of 10 nm AuNPs (300, 400, 500, 600, 700 μL) were mixed with 1 mL of pH 10 glycine–NaOH buffer, 50 μL of 500 μM TGA, and 50 μL of 1 μM Pb^{2+}, incubated for 10 minutes, and absorbance was measured over 400–800 nm. The optimum volume of 10 nm AuNPs was mixed with 1 mL of pH 10 glycine–NaOH buffer, 50 μL of 500 μM TGA, and 50 μL of 1 μM Pb^{2+}, incubated for various times (10, 20, 30, 40, 50, 60, 70, 80, 90, 100 minutes), and absorbance was measured over 400–800 nm. In the next step, 10 nm AuNPs (700 μL) was mixed with 1 mL of pH-optimal glycine–NaOH buffer, different TGA concentrations (10, 50, 100, 500, 1000 μM), and 50 μL of 1 μM Pb^{2+}, incubated for 10 minutes, and absorbance was measured over 400–800 nm. For the final optimization, 10 nm AuNPs (700 μL) were mixed with 1 mL of glycine–NaOH buffer at varying pH levels (8.6, 9.0, 9.6, 10.0, 10.6), 50 μL of 500 μM TGA, and 50 μL of 1 μM Pb^{2+}, incubated for 10 minutes, and absorbance was measured over 400–800 nm.[16]

2.5. Characterization of TGA-conjugated AuNPs

700 μL of 10 nm AuNPs was mixed with 1 mL of pH 10 glycine–NaOH buffer and 50 μL of 500 μM TGA, incubated for 10 minutes, and absorbance was measured over 400–800 nm. AuNPs and TGA-AuNPs were analyzed using IR spectroscopy in the range of 4000–500 cm^{-1}. The particle size distribution of AuNPs was analyzed using HRTEM. Samples of AuNPs and TGA-AuNPs/Pb^{2+} were placed on a copper grid, dried for 1 hour, and examined using HRTEM.

2.6. Sensitivity and selectivity tests of TGA-conjugated AuNPs

For the sensitivity test, 700 μL of 10 nm AuNPs was mixed with 1 mL of pH 10 glycine–NaOH buffer, followed by 50 μL of 500 μM TGA, and 50 μL varying concentrations of Pb^{2+} (0, 0.001, 0.01, 0.1, 10 μg mL^{-1}), then incubated for 10 minutes. Absorbance was measured over 400–800 nm. For the selectivity test, 700 μL of 10 nm AuNPs was mixed with 1 mL of pH 10 glycine–NaOH buffer and 50 μL of 500 μM TGA, followed by 50 μL of different metal ions (Ba^{2+}, Cu^{2+}, Hg^{2+}, Mg^{2+}, Mn^{2+}) at 9.5 μg mL^{-1}, incubated for 10 minutes, and absorbance was measured over 400–800 nm.

2.7. Application of TGA-conjugated AuNPs for Pb^{2+} detection in water samples

For the detection of Pb^{2+} in water samples, 100 μL of filtered lake water (filtered using 0.45 μm filter paper) was added to a synthesized TGA-AuNPs solution, which contained 700 μL of AuNPs, glycine–NaOH buffer, 50 μL of 500 μM TGA, and was maintained at pH 10.0 for 10 minutes. Subsequently, 50 μL of 0.01 μg per mL Pb^{2+} was added to the spiked lake water sample. The absorbance was measured and compared between the positive control and the lake water sample to determine the presence of Pb^{2+}.

3 Results and discussion

3.1. Characterization of AuNPs pre-and post-treatment

Gold nanoparticles (AuNPs) were characterized before and after treatment using UV-vis spectrophotometry to assess their optical properties and stability. The pre-treatment gold nanoparticles (AuNPs) were red. They exhibited a maximum absorbance at 520 nm as measured by UV-vis spectrophotometry (Fig. 1A). It indicates well-dispersed particles with an average diameter of 10–20 nm. This dispersion is attributed to the electrostatic repulsion from the negatively charged citrate layer weakly adsorbed on the AuNPs surface, enhancing their stability in aqueous solutions.[17,18] In the post-treatment solution, a red shift in absorption from 520 nm to 633 nm indicated aggregation of AuNPs into larger clusters (Fig. 1B). The SPR peak shifted depending on the interaction with thioglycolic acid (TGA) and the subsequent chelation with lead ions (Pb^{2+}), reflecting changes in particle size and aggregation state. Upon treatment with glycine–NaOH buffer, thioglycolic acid (TGA), and lead ions (Pb^{2+}), the gold nanoparticles (AuNPs) changed from a wine red to a bluish-purple color. This color shift results from plasmonic coupling due to chelation between TGA and Pb^{2+}, leading to the aggregation of TGA-AuNPs. The addition of Pb^{2+} ions facilitate chelation with the carboxylate groups on TGA-AuNPs, reducing the interparticle distance and inducing aggregation.[19] The specific interaction between TGA's

 © 2025 The Author(s). Published by the Royal Society of Chemistry

Open Access Article. Published on 03 March 2025. Downloaded on 11/8/2025 10:29:35 PM.
This article is licensed under a Creative Commons Attribution-NonCommercial 3.0 Unported Licence.

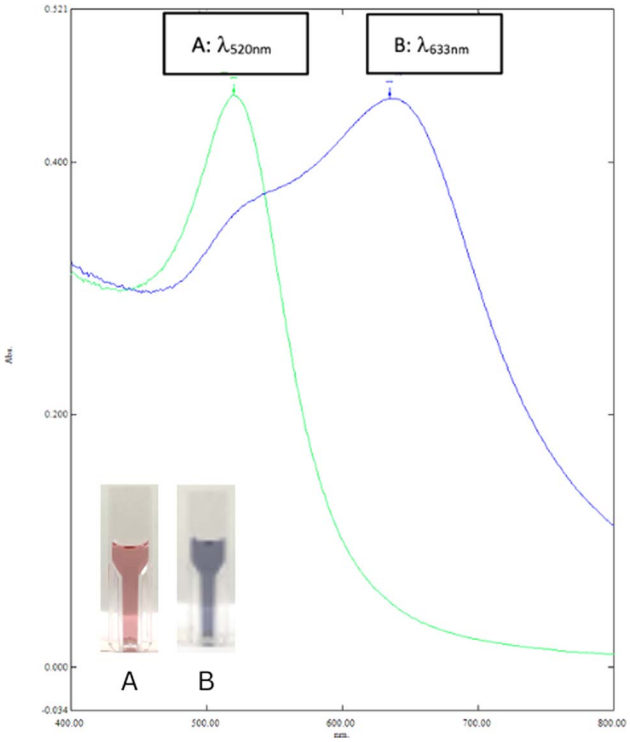

Fig. 1 UV-vis spectra of pre-treatment (A) of gold nanoparticles in water and post-treatment (B) of gold nanoparticles in the addition of 1 mL of pH 10.0 glycine–NaOH buffer, 50 μL of 500 μM TGA, and the presence of 50 μL of 1 μM Pb^{2+}.

carboxylate groups and Pb^{2+} forms TGA–Pb^{2+}–TGA linkages, contributing to this observable shift.[20]

3.2. Method optimization

Optimization of the synthesis parameters showed that a volume of 700 μL of AuNPs provided the best absorbance at 0.299 (Fig. 2A). The optimal reaction time was determined to be 10 minutes for the AuNPs-TGA/Pb^{2+} mixture, yielding the highest absorbance (Fig. 2B). A TGA concentration of 500 μM and a pH of 10.0 were identified as optimal (Fig. 2C and D), with the highest absorbance ratio A660/A520 observed at this pH, indicating better dispersion at a basic pH.

Optimization of the AuNPs involved varying parameters, such as the volume of nanoparticles and the incubation time, to achieve the highest absorbance and stability. The UV-vis spectra revealed that increasing the volume of AuNPs led to higher absorbance values, with an optimal volume identified at 700 μL. The concentration of gold nanoparticles, represented by the volume of AuNPs added, shows a direct linear relationship with absorbance, as expected from Beer–Lambert law ($A = C$). Linear regression equation of $y = 0.0409 + 0.0004x$ was derived with five concentrations tested, yielding an intercept of 0.0409 and a slope of 0.0004. The correlation coefficient was $r = 0.994$, with $r^2 = 0.9894$, fulfilling the ICH criteria for linearity ($r^2 \geq 0.98$).[21] This confirms the method's linearity and accuracy across the tested range.

The effect of incubation time on TGA-AuNPs/Pb^{2+} was evaluated by optimizing the incubation duration in the range of 10–100 min. TGA-AuNPs/Pb^{2+} at 10-minute incubation showed a result in the maximum absorbance, indicating complete aggregation of the nanoparticles. Between 20 and 70 minutes, the blue color faded to a lighter hue, and by 80 to 100 minutes, the mixture became clear with black particles forming, signaling uncontrolled aggregation. This indicates that the nanoparticles size exceeded the wavelength of light, disrupting surface plasmon resonance (SPR).[17] It was observed that longer reaction times led to decreased absorbance and increased aggregation, with data showing a visual decrease in absorbance over time. The observed aggregation was attributed to strong interparticle forces. Extended incubation resulted in a red shift and reduced absorbance, consistent with SPR theory, which explains that larger nanoparticles shift the maximum wavelength to longer values due to decreased excitation energy.

In the surface modification of AuNPs, the concentration of TGA directly influences the charge state of the nanoparticles and their surface plasmon resonance, impacting both stability and detection sensitivity. Thus, we investigated the effect of TGA concentration on the performance of the TGA-AuNPs sensor. At 10 μM and 50 μM, TGA did not induce significant color changes in the AuNPs mixture, which remained red with wavelength peaks around 515–520 nm, indicating insufficient aggregation. This suggests that lower concentrations of TGA are less effective in binding or aggregating AuNPs, potentially due to inadequate TGA per nanoparticle.[22] At TGA concentrations of 100 to 1000 μM, a clear progression in color from red to dark purple and then to blue was observed, indicating effective aggregation of AuNPs (Fig. 2C). However, at 1000 μM, absorbance decreased. Likely due to TGA replacing citrate on the AuNP surface and forming Au–S bonds, which reduced the surface charge and electrostatic repulsion between AuNPs. This decreased the stability of the nanoparticles with higher TGA concentrations. Therefore, 500 μM thioglycolic acid was chosen for the following experiments.

The pH conditions play a crucial role in colorimetric detection. The carboxylate groups ($-COO^-$) in thioglycolic acid are sensitive to pH variations, affecting the stability of nanoparticles.[23] Changes in pH can disrupt the stability of thioglycolic acid on gold nanoparticles, interfering with the electrostatic interactions between lead and TGA-AuNPs, thereby altering colorimetric and UV-vis responses.[24] We investigated the colorimetric response of TGA-AuNPs with Pb^{2+} at different pH (8.6, 9.0, 9.6, 10.0 and 10.6). The absorbance of the TGA-AuNPs solution for Pb^{2+} detection was poor at pH 8.6. Absorbance increased and reached a maximum at pH 10.0 before decreasing at pH 10.6 (Fig. 2D). This indicates that aggregation of AuNPs is minimal at acidic pH. At the same time, dispersion remains stable at basic pH. Conversely, citrate is fully deprotonated at neutral or basic pH, maintaining a negative surface charge that prevents aggregation.[23]

3.3. Characterization of TGA-conjugated AuNPs

TGA was conjugated to AuNPs to enhance their stability and functionality for lead ion detection. The conjugation was confirmed by the UV-vis absorbance shift from 520 nm to a longer wavelength upon adding TGA and Pb^{2+}, indicating successful functionalization and particle aggregation. The TGA

Open Access Article. Published on 03 March 2025. Downloaded on 11/8/2025 10:29:35 PM.
This article is licensed under a Creative Commons Attribution-NonCommercial 3.0 Unported Licence.

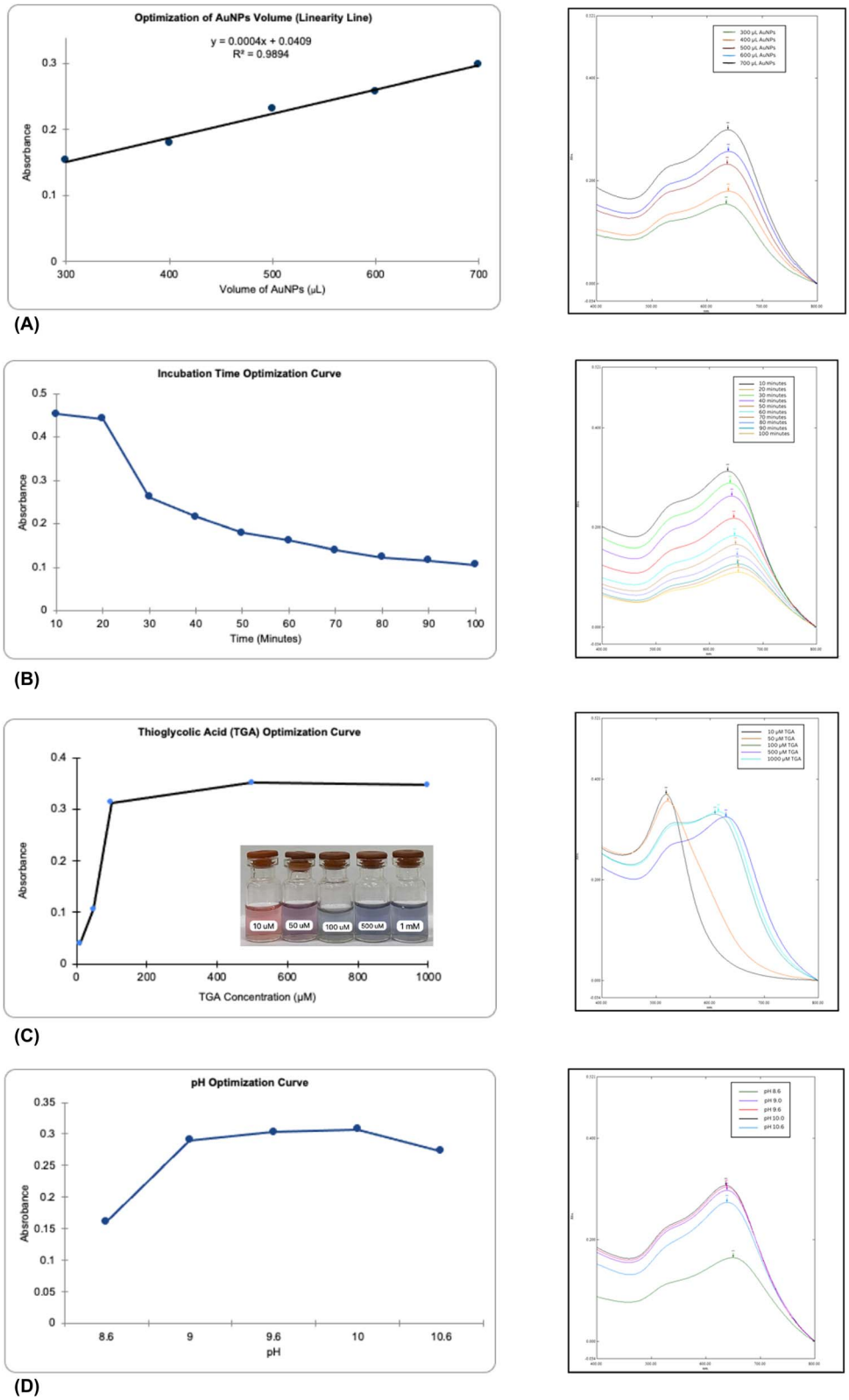

Fig. 2 UV-vis absorption spectra of different AuNPs volume (300, 400, 500, 600, 700 μL) (A); different incubation time (10, 20, 30, 40, 50, 60, 70, 80, 90, 100 minutes) (B) different TGA concentration 10, 50, 100, 500, 1000 μM (C), and different pH (8.6, 9.0, 9.6, 10.0, 10.6) (D).

 © 2025 The Author(s). Published by the Royal Society of Chemistry

Open Access Article. Published on 03 March 2025. Downloaded on 11/8/2025 10:29:35 PM.
This article is licensed under a Creative Commons Attribution-NonCommercial 3.0 Unported Licence.

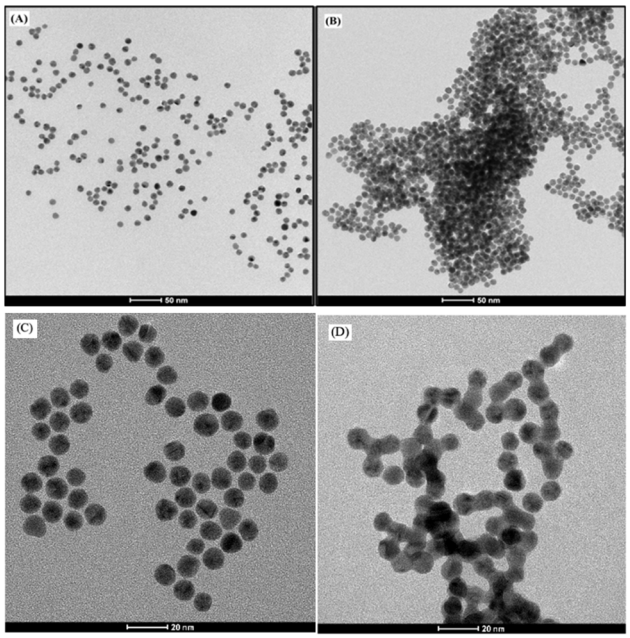

Fig. 3 TEM images of AuNPs (A), AuNPs-TGA/Pb^{2+} (B) and HRTEM images of AuNPs (C), AuNPs-TGA/Pb^{2+} (D) in the presence of 1 μM Pb^{2+}.

provided strong covalent bonds through its thiol groups, enhancing the stability and ensuring the nanoparticles remained well-dispersed.

TEM analysis was used to assess morphological changes in AuNPs before and after conjugation with TGA and Pb^{2+}. Initially, the TEM and HRTEM images (Fig. 3A and C) showed that the unconjugated AuNPs were predominantly uniform, spherical, and mostly monodispersed, with an average diameter of 10.39 nm. After the addition of TGA and Pb^{2+}, the TEM and HRTEM images (Fig. 3B and D) showed that the AuNPs had increased aggregation and formed clusters, with an average diameter of 11.02 nm, indicating a size increase of 0.63 nm. This increase suggests that Pb^{2+} ions interact with the carboxylate groups of TGA adsorbed on the nanoparticle surface, promoting aggregation and altering particle size and distribution.[25]

FTIR characterization was performed to investigate the binding interactions between AuNPs and TGA. The spectrum of pure TGA solution (Fig. 4A) shows distinctive functional groups, including a thiol group (S–H) absorption peak at 2567.02 cm^{-1} and carboxyl group features identified by a C=O stretch at 1698.29 cm^{-1}, an O–H stretch at 3005.92 cm^{-1}, and an overlapping C–H stretch at 2924.03 cm^{-1}.[18,26] In the AuNPs-TGA spectrum (Fig. 4B), the disappearance of the S–H peak confirms the formation of Au–S bonds. Additionally, red and blue shifts in the C=O and O–H peaks, respectively, suggest molecular interactions altering vibrational modes due to TGA binding, replacing citrate ions on the AuNPs surface and leaving the carboxyl group free.[24] These spectral changes indicate successful conjugation of TGA to AuNPs, confirming the interaction mechanism proposed.[18]

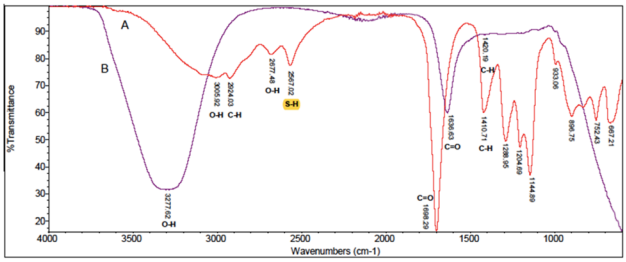

Fig. 4 FTIR images of thioglycolic acid (A) and TGA-AuNPs (B).

3.4. Sensitivity and selectivity tests of TGA-conjugated AuNPs

Sensitivity tests were conducted using gold nanoparticles (AuNPs) with optimal conditions of 700 μL AuNPs, 500 μM TGA, and a pH of 10.0 with a 10-minute incubation. The maximum permissible lead concentration in drinking water by EPA is 15. To evaluate sensitivity, various lead concentrations (10, 1, 0.1, 0.01, 0.001 μg mL^{-1}, and 0 μg mL^{-1} control) were tested. Absorbance measurements were taken using the $A_{633/520}$ nm ratio, enhancing accuracy by minimizing interference from other substances and specifically reflecting changes due to lead.

The limit of detection (LOD) of this method, calculated from the calibration curve, was 9.5 μg mL^{-1} (Fig. 5A). This method is less sensitive than that by Chai *et al.* (2010) using glutathione, which had an LOD of 20.72 μg L^{-1}.[11] Glutathione's two free

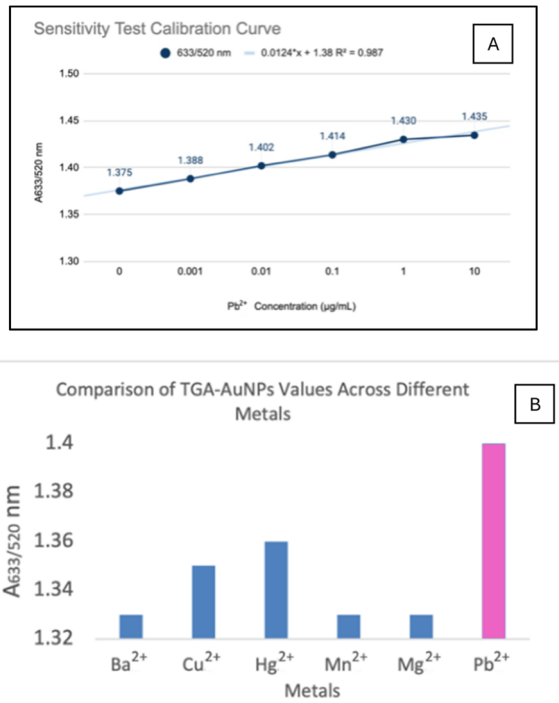

Fig. 5 Sensitivity in various Pb^{2+} concentration (10, 1, 0.1, 0.01, 0.001 μg mL^{-1}, and 0 μg mL^{-1} control) (A) and selectivity (B) of the method for Pb^{2+} detection when compared to different metal ions (Ba^{2+}, Cu^{2+}, Hg^{2+}, Mg^{2+}, Mn^{2+}) at 9.5 μg mL^{-1}.

Open Access Article. Published on 03 March 2025. Downloaded on 11/8/2025 10:29:35 PM.
This article is licensed under a Creative Commons Attribution-NonCommercial 3.0 Unported Licence.

Table 1 One way Anova statistical test results between reference metals and Pb^{2+}

	Sum of squares	df	Mean square	F	Sig.
Between groups	0.012	5	0.002	4.116×10^{14}	0.000
Within groups	0.000	12	0.000		
Total	0.012	17			

carboxylic groups likely contribute to its higher sensitivity than thioglycolic acid, which has only one. However, the method is more sensitive than Kim *et al.* (2001), which used 11-MUA with an LOD of 400 μM (82.88 μg mL^{-1}).[10] This proves that the shorter the chain length of the conjugate, the higher the sensitivity of the method.

The selectivity test showed that the absorbance ratio for Pb^{2+} was significantly higher than for other metals (Ba^{2+}, Cu^{2+}, Hg^{2+}, Mn^{2+}, Mg^{2+}) (Fig. 5B), with statistically significant differences ($p < 0.05$). All ions caused a color change to blue, similar to Pb^{2+}, indicating that visual selectivity is limited. Spectrophotometric analysis revealed absorbance values above 0.2 for all six metals, with Pb^{2+} showing superior absorbance compared to the others.

The one-way ANOVA results demonstrate significant differences in absorbance ratios among various metals (Table 1), and the LSD test confirms that Pb^{2+} has a notably higher absorbance ratio compared to the other metals (Table 2). One-way ANOVA was performed to evaluate the significance of absorbance differences among the metals. The analysis yielded a p-value of 0.0001 (<0.05), confirming significant differences. Post Hoc testing using Least Significant Difference (LSD) with an LSD value of 0.017 identified Pb^{2+} as significantly different from the other metals. The ratios of Pb^{2+} to Ba^{2+}, Cu^{2+}, Hg^{2+}, Mn^{2+}, and Mg^{2+} were 0.074, 0.047, 0.035, 0.073, and 0.065, respectively, all exceeding the BNT value.

These results demonstrate that the developed method is relatively selective for Pb^{2+} compared to other tested metals, although visual inspection alone does not provide clear selectivity due to similar color changes. Apart from that, another limitation is the selectivity testing carried out on individual metal ions. However, despite its limitations, the method is more selective than previous approaches using glutathione, which required a higher metal concentration (50 μM). It also shows improved selectivity over methods using 11-MUA, which only tested three metals and had limitations in distinguishing Pb^{2+} from Hg^{2+} and Cd^{2+}.[10,11] Furthermore, the method's selectivity is confirmed quantitatively through absorbance ratio comparisons.

Table 2 Calculation results of LSD values between reference metals and Pb^{2+}

Calculation	
MSE	0.0001
t (α, df_e)	2.17881283
α	0.05
df_e	12
r	3
LSD	0.01778993226

Table 3 Pb^{2+} detection in water lake samples

Sources	Pb^{2+}	$A_{633/520}$
Kenanga lake	Unspiked	1.298
	Spiked 0.01 μg mL^{-1}	1.380
Puspa lake	Unspiked	1.333
	Spiked 0.01 μg mL^{-1}	1.386
FMIPA lake	Unspiked	1.345
	Spiked 0.01 μg mL^{-1}	1.475

3.5. Application of TGA-conjugated AuNPs for Pb^{2+} detection in water samples

The colorimetric AuNPs-TGA method effectively detected Pb^{2+} in lake water samples, showing higher absorbance ratios after Pb^{2+} addition compared to samples without Pb^{2+} (Table 3). This indicates the method's efficacy for lead detection in water samples.

The practical application of TGA-conjugated AuNPs was demonstrated by testing their ability to detect Pb^{2+} in water samples from the University of Indonesia. The lake water samples, containing various organic and inorganic contaminants, were ideal for evaluating the colorimetric method's effectiveness in detecting Pb^{2+}. Water from Kenanga Lake, Puspa Lake, and FMIPA Lake was filtered through a 0.45 μm membrane. To test the method's capability in complex matrices, known quantities of Pb^{2+} were spiked into the samples and analyzed using UV-vis spectrophotometry.

The results showed that the absorbance ratios ($A_{633/520}$) for the lake samples without added Pb^{2+} were lower than those spiked with 0.01 μg per mL Pb^{2+}. Regression analysis indicated negative values for Pb^{2+} concentration in unspiked samples, suggesting that the Pb^{2+} levels were below the detection limit of the AuNPs-TGA method. Furthermore, the color of the lake water samples shifted from purple to gray without added Pb^{2+}, supporting the method's potential for qualitative and quantitative Pb^{2+} detection in water. The nanoparticles effectively detected Pb^{2+} at low concentrations, with a spectral response, proving to be a tool for environmental monitoring.

4 Conclusions

This study successfully identified the optimal conditions for synthesizing TGA-AuNPs as a Pb^{2+} sensor. The optimal synthesis parameters included using 700 μL of gold nanoparticles with 500 μM thioglycolic acid at pH 10.0 for 10 minutes. However, the lowest detectable Pb^{2+} concentration achieved was 9.5 μg mL^{-1}. Despite demonstrating superior selectivity for Pb^{2+} over other tested metals, further

 © 2025 The Author(s). Published by the Royal Society of Chemistry

Open Access Article. Published on 03 March 2025. Downloaded on 11/8/2025 10:29:35 PM.
This article is licensed under a Creative Commons Attribution-NonCommercial 3.0 Unported Licence.

improvements in sensitivity are necessary for the practical application of TGA-AuNPs as a colorimetric sensor in water.

Data availability

No new data were reffered or analysed as part of this manuscript.

Author contributions

Febrina Amelia Saputri – conceptualization, methodology, original draft preparation, funding acquisition; Talitha Shabirah Aulia – draft preparation, formal analysis; Catur Jatmika – methodology, review and editing; Raditya Iswandana – review and editing; Sandra Megantara – review and editing; Vinayak A. Dhumale – methodology, review and editing.

Conflicts of interest

There are no conflicts to declare.

Acknowledgements

This project was funded by Ministry of Education, Culture, Research, and Technology, Indonesia (051/E5/PG.02.00.PL/2024, 350/PKS/WR III/UI/2024, and NKB-817/UN2.RST/HKP.05.00/2024).

References

1 J. Briffa, E. Sinagra and R. Blundell, *Heliyon*, 2020, **6**, e04691.
2 World Health Organization, Lead poisoning, **https://www.who.int/news-room/fact-sheets/detail/lead-poisoning-and-health**, (accessed 28 August 2024).
3 R. D. P. Astuti, A. Mallongi, R. Amiruddin, M. Hatta and A. U. Rauf, *Gac. Sanit.*, 2021, **35**, S33–S37.
4 G. Prayoga, B. A. Utomo and H. Effendi, *Biotropia*, 2022, **29**(1), 7–17.
5 N. Ratnarathorn, O. Chailapakul and W. Dungchai, *Talanta*, 2015, **132**, 613–618.
6 B. Sarkar and P. Mondal, *J. Water Environ. Nanotechnol.*, 2021, **6**, 22–40.
7 F. A. Saputri, E. U. Zubaidah, A. W. P. Kenanga, C. Jatmika, R. Pratiwi and V. A. Dhumale, *Molecules*, 2023, **28**, 6527.
8 E. Priyadarshini and N. Pradhan, *Sens. Actuators, B*, 2017, **238**, 888–902.
9 Y.-L. Hung, T.-M. Hsiung, Y.-Y. Chen and C.-C. Huang, *Talanta*, 2010, **82**, 516–522.
10 Y. Kim, R. C. Johnson and J. T. Hupp, *Nano Lett.*, 2001, **1**, 165–167.
11 F. Chai, C. Wang, T. Wang, L. Li and Z. Su, *ACS Appl. Mater. Interfaces*, 2010, **2**, 1466–1470.
12 Centers for Disease Control and Prevention, Lead Toxicity, **https://www.atsdr.cdc.gov/csem/leadtoxicity/safety_standards.html#:~:text=OSHAsetaPermissibleExposure,than30daysperyear**, (accessed 28 August 2024).
13 OECD, Thioglycolic acid and its ammonium salt, **https://hpvchemicals.oecd.org/ui/handler.axd?id=561455be-de6f-4d2e-b38c-8137b71c577d**, (accessed 28 August 2024).
14 A. S. Andreani, S. Suyanta, E. S. Kunarti and S. J. Santosa, *Indones. J. Chem.*, 2018, **18**, 434.
15 C. Fan, S. He, G. Liu, L. Wang and S. Song, *Sensors*, 2012, **12**, 9467–9475.
16 J. Gahlaut, Y. S. Rajput, S. Meena, D. K. Nanda and R. Sharma, *Anal. Lett.*, 2018, **51**, 1208–1218.
17 Z. Sadiq, S. H. Safiabadi Tali, H. Hajimiri, M. Al-Kassawneh and S. Jahanshahi-Anbuhi, *Crit. Rev. Anal. Chem.*, 2023, 1–36.
18 D. K. Nguyen and C.-H. Jang, *Anal. Biochem.*, 2022, **645**, 114634.
19 C. Fan, S. He, G. Liu, L. Wang and S. Song, *Sensors*, 2012, **12**, 9467–9475.
20 J. A. Flowers, M. J. Farrell, G. Rutherford and A. K. Pradhan, *Biosensors*, 2023, **13**, 819.
21 European Medicines Agency, ICH guideline Q2(R2) on validation of analytical procedures, **https://www.ema.europa.eu/en/documents/scientific-guideline/ich-guideline-q2r2-validation-analytical-procedures-step-2b_en.pdf**, (accessed 29 August 2024).
22 Z. Liu, J. Hu, S. Tong, Q. Cao and H. Yuan, *Spectrochim. Acta, Part A*, 2012, **97**, 737–740.
23 M. Annadhasan, T. Muthukumarasamyvel, V. R. Sankar Babu and N. Rajendiran, *ACS Sustain. Chem. Eng.*, 2014, **2**, 887–896.
24 H. Zhang, Y. Qu, Y. Zhang, Y. Yan and H. Gao, *Anal. Methods*, 2022, **14**, 1996–2002.
25 W. Ghann, T. Harris, D. Kabir, H. Kang, M. Jiru, M. M. Rahman, M. M. Ali and J. Uddin, *J. Nanomed. Nanotechnol.*, 2019, **10**(6), DOI: **10.35248/2157-7439.19.10.539**.
26 D. L. Andrews, in *Encyclopedia of Spectroscopy and Spectrometry*, Elsevier, 1999, pp. 397–401.